

# Design of Decentralized IMC-PID Controller Based on dRI Analysis

Mao-Jun He, Wen-Jian Cai, and Bing-Fang Wu

School of Electrical and Electronic Engineering, Nanyang Technological University, Singapore 639798

DOI 10.1002/aic.10994

Published online October 4, 2006 in Wiley InterScience (www.interscience.wiley.com).

*A simple yet effective method for designing decentralized PID controller, which is based on dynamic interaction analysis and internal model control principle, is proposed. On the basis of structure decomposition, the dynamic relative interaction is defined and represented by the process model and controller explicitly. Using the initial controllers designed for the diagonal elements, the multiplicate model factor is derived, and then simplified to a pure time delay function at the neighborhood of each control loop critical frequency to obtain the equivalent transfer function for the particular control loop. Consequently, appropriate parameters of individual controller are determined by applying the IMC-PID tuning rules for the equivalent-transfer function. Simulation results for a variety of  $2 \times 2$ ,  $3 \times 3$  and  $4 \times 4$  systems show that the design technique results better overall control performance than those of existing design methods. © 2006 American Institute of Chemical Engineers AIChE J, 52: 3852–3863, 2006*

**Keywords:** multivariable processes, decentralized control, internal model control, PID, dynamic relative interaction, multiplicate model factor, simulation

## Introduction

Design of multiple-input multi-output (MIMO) control systems have received a great deal of attention in the control literature. In spite of the availability of sophisticated methods for designing centralized control systems, decentralized proportional-integral-derivative (PID) control is still the most commonly used technique in the process control industries for control of multivariable processes. The main reasons for such popularity are that PID controllers are easily understandable by control engineers and the decentralized PID controllers require fewer parameters to tune than that of multivariable controllers. Another advantage of the decentralized PID controllers is that loop failure tolerance of the resulting closed-loop control system can be guaranteed at the design stage. Even though the design and tuning of single loop PID controllers have been extensively researched,<sup>1,2,3,4</sup> they cannot be directly applied to design decentralized control systems due to the existence of

interactions among control loops. Many methods had been proposed to extend SISO PID tuning rules to decentralized control by compensating the effects of loop interactions. A common way is to first design individual controller for each control loop by ignoring all interactions, and then detune each loop by a detuning factor. Luyben proposed the biggest log modulus tuning (BLT) method for multiloop PI controllers.<sup>5,6</sup> In the BLT method, the well known Ziegler-Nichols rule is modified with the inclusion of a detuning factor, which determines the tradeoff between stability and performance of the system. Similar methods have also been addressed by Chien et al.<sup>7</sup> There, the designed PID controllers for the diagonal elements are detuned according to the relative gain array (RGA) values. Despite simple computations involved, the design regards interactions as elements obstructing system stability, and attempts to dispose of them rather than control them to increase the speed of individual control loops. It is, hence, too conservative to exploit process structures and characteristics for best achievable performance. Lee et al.<sup>8</sup> proposed a method to improve multiloop PI/PID control system via adjusting the dominant pole or the peak amplitude ratio. However, the design procedures for obtaining the less conservative detuning factors

Correspondence concerning this article should be addressed to W.-J. Cai at ewjcai@ntu.edu.sg.

are complex and require higher calculation load. In the sequential loop closing method,<sup>9,10</sup> by taking interactions from the closed loops into account in a sequential fashion, multiple single-loop design strategies can be directly employed. The main drawback of this method is that the design must proceed in a very *ad hoc* manner. Design decisions made when the first one or two loops are closed may have deleterious effects on the behavior of the remaining loops. The interactions are well taken care of only if the loops are of considerably different bandwidths and the closing sequence starts from the fastest loop.

In recent years, the new trend in designing decentralized control system for multivariable processes is to handle the loop interactions first, and then apply SISO PID tuning rules. The independent design methods have been used by several authors, in which each controller is designed based on the paired transfer functions, while satisfying some constraints due to the loop interactions.<sup>11,12</sup> The constraints imposed on the individual loop are given by criteria such as the  $\mu$ -interaction measure,<sup>13</sup> and the Gershgorin bands.<sup>14</sup> Usually, stability and failure tolerance are automatically satisfied. Since the detailed information on controller dynamics in other loops is not used, the resulting performance may be poor.<sup>9</sup> In the trial-and-error method,<sup>15</sup> Lee et al. extended the iterative continuous cycling method for SISO systems to decentralized PI controller tuning. It refined the Nyquist array method to provide less conservative stability conditions, and ultimate gains for decentralized tuning are then determined. The main disadvantages are not only due to the need for successive experiments but also the weak tie between the tuning procedure and the loop performance. To overcome the difficulty of controllers interact with each other, Wang et al.<sup>16</sup> used a modified Ziegler-Nichols method to determine the controller parameters that will give specified gain margins. Although it presents an interesting approach, design of multiloop controller by simultaneously solving a set of equations is numerically difficult. Huang et al.<sup>17</sup> formulated the effective transmission in each equivalent loop as the effective open-loop process (EOP), the design of controllers can then be carried out without referring to the controller dynamics of other loops. However, for high-dimensional processes, the calculation of EOPs is complex, and the controllers have to be conservative for the inevitable modeling errors encountered in formulation.

In this article, a simple yet effective decentralized PID controller design methodology is proposed based on dynamic interaction analysis and internal model control principle. On the basis of structure decomposition, the dynamic relative interaction is defined and represented by the process model and controller explicitly. An initial decentralized controller is designed first by using the diagonal elements and then implemented to estimate the dynamic relative interaction (dRI) to individual control loop from all others. With the obtained dRI, the multiplicate model factor is derived, and then simplified to

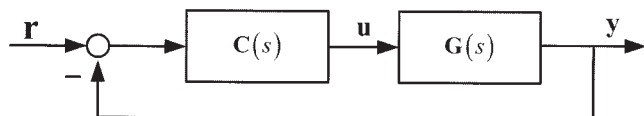


Figure 1. General decentralized control system.

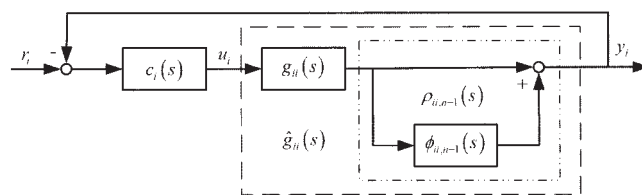


Figure 2. Structure of loop  $y_i - u_i$  by structural decomposition.

a pure time delay function at the neighborhood of each control loop critical frequency to obtain the equivalent transfer function for the particular control loop. Consequently, appropriate controller parameters for individual control loop are determined by applying the IMC-PID tuning rules for the equivalent transfer function. Examples for a variety of  $2 \times 2$ ,  $3 \times 3$  and  $4 \times 4$  systems are used to demonstrate that the overall control system performance is much better than that of other tuning methods, such as the BLT method,<sup>5,6</sup> the trial and error method,<sup>15</sup> and the independent design method based on Nyquist stability analysis,<sup>14</sup> especially for higher-dimensional processes.

## Preliminaries

Consider an  $n \times n$  system with a decentralized feedback control structure as shown in Figure 1, where,  $\mathbf{r}$ ,  $\mathbf{u}$  and  $\mathbf{y}$  are vectors of references, inputs and outputs respectively,  $\mathbf{G}(s) = [g_{ij}(s)]_{n \times n}$  is system's transfer-function matrix with its individual element  $g_{ij}(s)$  described by the common used models, as given by the second column in Table 1, and controller  $\mathbf{C}(s) = \text{diag}\{c_1(s), \dots, c_n(s)\}$  is the decentralized PID type with its individual element given in parallel form as

$$c_i(s) = k_{pi} \left( 1 + \frac{1}{\tau_{is}s} + \tau_{di}s \right) \quad (1)$$

It is assumed that  $\mathbf{G}(s)$  has been arranged so that the pairings of the inputs and outputs in the decentralized feedback system correspond to the diagonal elements of  $\mathbf{G}(s)$ .

For multi-input multi-output (MIMO) process, when one controller,  $c_i(s)$ , acting in response to the setpoint change and/or the output disturbance, it affects the overall system through the off-diagonal elements of  $\mathbf{G}(s)$ , forcing other controllers to take actions, as well, these controllers reversely influence the  $i$ th loop via other off-diagonal elements, and this interacting processes among control loops continue throughout the whole transient until a steady state is reached. To examine the transmittance of interactions between an individual control loop, and the others, the decentralized control system can be structurally decomposed into  $n$  individual SISO control loops with the coupling among all loops explicitly exposed and embedded in each loop. Figure 2 shows the structure of an arbitrary control loop  $y_i - u_i$  after the structural decomposition.

In Figure 2, the interaction to an individual control loop  $y_i - u_i$  from the other  $n - 1$  control loops is represented by the Relative Interaction (RI)  $\phi_{ii,n-1}(s)$ , and the equivalent-transfer function of an individual control loop  $y_i - u_i$ , denoted by  $\hat{g}_{ii}(s)$ , can be obtained in terms of  $\phi_{ii,n-1}(s)$  by

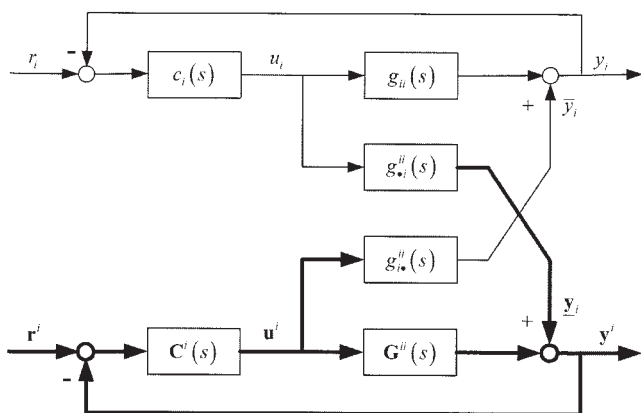


Figure 3. Closed-loop system with control loop  $y_i - u_i$  presented explicitly.

$$\hat{g}_{ii}(s) = g_{ii}(s)\rho_{ii,n-1}(s) \quad (2)$$

with

$$\rho_{ii,n-1}(s) = 1 + \phi_{ii,n-1}(s) \quad (3)$$

where  $\rho_{ii,n-1}(s)$  is defined as multiplicate model factor (MMF) to indicate the model change of an individual control loop  $y_i - u_i$  after the other  $n - 1$  control loops are closed. Once the RI,  $\phi_{ii,n-1}(s)$ , is available, the corresponding MMF,  $\rho_{ii,n-1}(s)$ , and the equivalent process transfer function  $\hat{g}_{ii}$  can be obtained which can be directly used to independently design the PID controller for each individual control loop  $y_i - u_i$ .

In the following development, we use RI as a basic interaction measure to investigate the interactions among control loops and derive equivalent-transfer function for each loop. Sometimes, we will omit the Laplace operator  $s$  for simplicity unless otherwise specified.

The RI for control loop  $y_i - u_j$  is defined as the ratio of two elements<sup>18</sup>: the increment of the process gain after all other control loops are closed, and the apparent gain in the same loop when all other control loops are open, that is

$$\phi_{ij,n-1} = \frac{(\partial y_i / \partial u_j)_{y_k \neq \text{constant}} - (\partial y_i / \partial u_j)_{u_l \neq \text{constant}}}{(\partial y_i / \partial u_j)_{u_l \neq \text{constant}}} \quad k, l = 1, \dots, n$$

Since the RI cannot offer effective measure on the reverse effect of individual control loop and loop-by-loop interactions, He and Cai decomposed the RI as the elements summation of decomposed relative interaction array (DRIA) to give important insights into the cause-effects of loop interactions.<sup>19</sup> However, the obtained results are limited to the steady state, which are less useful for controller design than the dynamic representations. Hence, it is necessary to derive the dynamic interaction among control loops represented explicitly by the process models and controllers.

### Dynamic Relative Interaction

As the dynamic interactions among control loops are controller dependent,<sup>20,21,22,23</sup> appropriate controllers have to be designed and implemented into the control system for investi-

gating the dynamic interactions. For an arbitrarily decentralized PID control system, we can redraw Figure 1 as Figure 3 for the convenience of analyzing the interactions between an arbitrary control loop  $y_i - u_i$  and the others, where  $\underline{y}_i$  is a vector indicating the effects of  $u_i$  to other outputs, while  $\bar{y}_i$  indicates the reverse effect of  $y_i$  by all the other closed control loops,  $\underline{r}^i$ ,  $\underline{u}^i$ ,  $\underline{y}^i$  and  $\underline{G}^i(s)$  indicate  $\underline{r}$ ,  $\underline{u}$ ,  $\underline{y}$  and  $\underline{C}(s)$  with their  $i$ th elements,  $r_i$ ,  $u_i$ ,  $y_i$  and  $c_i(s)$ , been removed, respectively.

Since the dynamic relative interaction are input independent, without loss of generality, the references of the other  $n - 1$  control loops are set as constants, that is

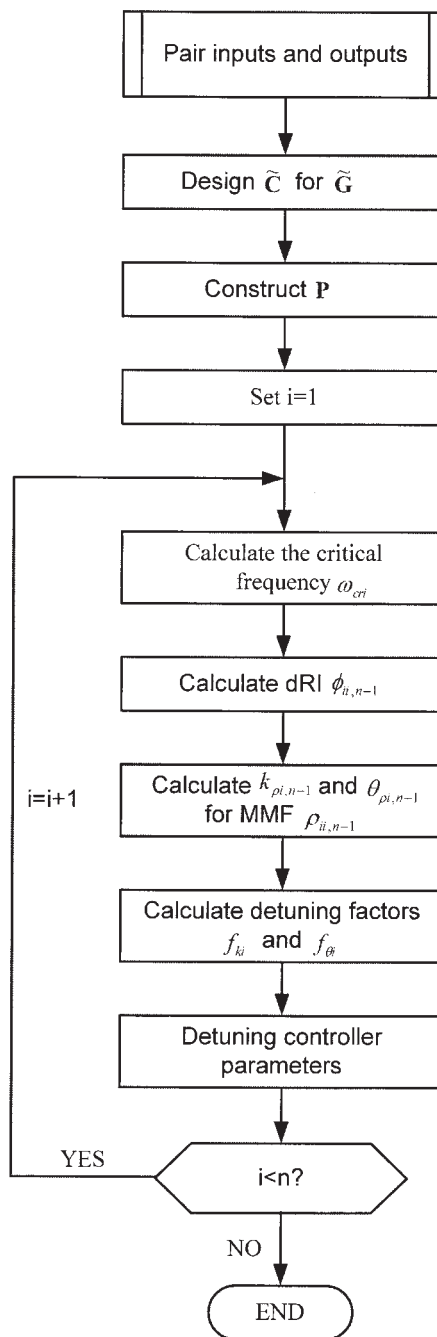
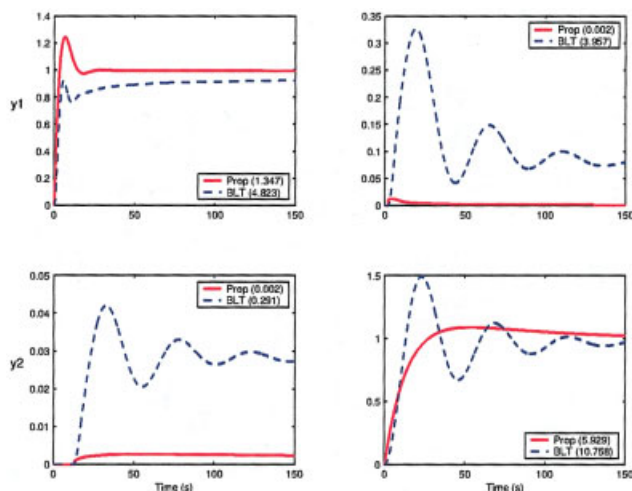


Figure 4. Procedure for designing decentralized PID controller.



**Figure 5. Step response and ISE values of decentralized control for Tyreus stabilizer (solid line: Proposed design, dashed line: BLT design, dashed-dotted line: Lee et al., dotted line: Chen et al.).**

[Color figure can be viewed in the online issue, which is available at [www.interscience.wiley.com](http://www.interscience.wiley.com).]

$$\frac{d\mathbf{r}_k}{dt} = 0 \quad \text{or} \quad \mathbf{r}_k(s) = 0, \quad k = 1, \dots, n; k \neq i,$$

in analysis of the dynamic interaction between control loop  $y_i - u_i$ , and the other controlled closed-loops. Then, we have

$$\mathbf{y}^i = \mathbf{G}^{ii} \mathbf{u}^i + \mathbf{y}_i \quad (4)$$

$$\mathbf{u}^i = -\mathbf{C}^i \mathbf{y}^i, \quad (5)$$

and

$$\mathbf{y}_i = g_{ii}^{ii} u_i \quad (6)$$

$$\bar{\mathbf{y}}_i = g_{ii}^{ii} \mathbf{u}^i \quad (7)$$

where  $\mathbf{G}^{ii}$  is the transfer function matrix  $\mathbf{G}$ , with its  $i$ th row, and the  $i$ th column removed, and  $g_{ii}^{ii}$  and  $g_{ii}^{ii}$  indicate the  $i$ th row, and the  $i$ th column of  $\mathbf{G}$  with the  $ii$ th element,  $g_{ii}$  removed, respectively.

Combining Eqs. 4 and 5, we can write

$$\mathbf{u}^i = -(\bar{\mathbf{G}}^{ii})^{-1} \mathbf{y}_i \quad (8)$$

where

$$\bar{\mathbf{G}} = \mathbf{G} + \mathbf{C}^{-1} \quad (9)$$

Furthermore,  $\bar{\mathbf{y}}_i$  in Eq. 7 can be represented by the summation of the following row vector

$$\bar{\mathbf{y}}_i = \left\| \begin{bmatrix} g_{i1} u_1 & \dots & g_{ik} u_k & \dots & g_{in} u_n \end{bmatrix} \right\|_{\Sigma}, \quad k = 1, \dots, n; k \neq i \quad (10)$$

where  $\|\mathbf{A}\|_{\Sigma}$  is the summation of all elements in a matrix  $\mathbf{A}$ .

Using Eqs. 6–10, we obtain

$$\begin{aligned} \bar{\mathbf{y}}_i &= \left\| -g_{ii}^{ii} (\bar{\mathbf{G}}^{ii})^{-1} g_{ii}^{ii} \right\|_{\Sigma} * u_i = \left\| -g_{ii}^{ii} g_{ii}^{ii} \otimes (\bar{\mathbf{G}}^{ii})^{-T} \right\|_{\Sigma} * u_i \\ &= \left\| -\frac{g_{ii}^{ii} g_{ii}^{ii}}{g_{ii}} \otimes (\bar{\mathbf{G}}^{ii})^{-T} \right\|_{\Sigma} * g_{ii} u_i \end{aligned}$$

Consequently, those steady-state relationships provided in reference 20 can be extended as following.

Define

$$\Delta \mathbf{G}_{ii,n-1} = -\frac{1}{g_{ii}} g_{ii}^{ii} g_{ii}^{ii}$$

as the incremental process gain matrix of subsystem  $\mathbf{G}^{ii}$  when control loop  $y_i - u_i$  is closed, then the dynamic DRIA (dDRIA) of individual control loop  $y_i - u_i$  in  $n \times n$  system can be described as

$$\Psi_{ii,n-1} = \Delta \mathbf{G}_{ii,n-1} \otimes (\bar{\mathbf{G}}^{ii})^{-T} \quad (11)$$

and the corresponding dynamic relative interaction (dRI),  $\phi_{ii,n-1}$ , is the summation of all elements of  $\Psi_{ii,n-1}$ , that is

$$\phi_{ii,n-1} = \|\Psi_{ii,n-1}\|_{\Sigma} = \|\Delta \mathbf{G}_{ii,n-1} \otimes (\bar{\mathbf{G}}^{ii})^{-T}\|_{\Sigma}, \quad (12)$$

where  $\otimes$  is the hadamard product, and  $[\mathbf{G}^{ij}]^{-T}$  is the transpose of the inverse of matrix  $\mathbf{G}^{ij}$ . From Eq. 9,  $\bar{\mathbf{G}}$  can be factorized as

$$\bar{\mathbf{G}} = \begin{pmatrix} g_{11} + 1/c_1 & g_{12} & \dots & g_{1n} \\ g_{21} & g_{22} + 1/c_2 & \dots & g_{2n} \\ \vdots & \vdots & \ddots & \vdots \\ g_{n1} & g_{n2} & \dots & g_{nn} + 1/c_n \end{pmatrix} = \mathbf{G} \otimes \mathbf{P},$$

where

$$\mathbf{P} = \begin{pmatrix} \frac{1 + g_{11}c_1}{g_{11}c_1} & 1 & \dots & 1 \\ 1 & \frac{1 + g_{22}c_2}{g_{22}c_2} & \dots & 1 \\ \vdots & \vdots & \ddots & \vdots \\ 1 & 1 & \dots & \frac{1 + g_{nn}c_n}{g_{nn}c_n} \end{pmatrix}. \quad (13)$$

Hence, the dDRIA and dRI can be obtained respectively by,

$$\Psi_{ii,n-1} = \Delta \mathbf{G}_{ii,n-1} \otimes (\mathbf{G}^{ii} \otimes \mathbf{P}^i)^{-T} \quad (14)$$

and

$$\phi_{ii,n-1} = \|\Delta \mathbf{G}_{ii,n-1} \otimes (\mathbf{G}^{ii} \otimes \mathbf{P}^i)^{-T}\|_{\Sigma} \quad (15)$$

**Remark 1:** In dDRIA and dRI of Eqs. 14 and 15, there exists an additional matrix  $\mathbf{P}$ , which explicitly reveals interactions to an arbitrary loop by all the other  $n - 1$  closed loops under band limited control conditions. Thus, for the given decentralized PID controllers, the dynamic interaction among control loops at an arbitrary frequency can be easily investigated through the matrix  $\mathbf{P}$ , moreover, the calculation remains simple even for high-dimensional processes.

**Remark 2:** For decentralized PI or PID control, we have

$$\mathbf{C}^{-1}(j0) = \mathbf{0},$$

and

$$\bar{\mathbf{G}}(j0) = \mathbf{G}(j0)$$

which implies that the RI and the dRI are equivalent at steady state. However, since the dRI measure interactions under practical imperfect control conditions at some specified frequency points, it is more accurate in estimating the dynamic loop interactions, and more effective in designing decentralized controllers.

The significance of the above development are:

1. The interaction to individual control loop from the other loops is derived in matrix form, and the relationship between RI and DRIA is extended to the whole frequency domain from the steady state;

2. Equations 11 and 12 indicate the dRI is a combination of the interactions to individual control loop from the others, and loop pairings selected based on the dRI may be inaccurate as there may exist cause-effect cancelation among them such that<sup>19</sup>;

3. As interactions among control loops are controllers dependent, the dDRIA represents how the decentralized controllers interact with each other, while the dRI provides the overall effect to individual control loop from the others;

4. The dRI can be obtained easily once process transfer function elements and controllers are available, which is not limited by the system dimension.

## Estimation of Equivalent Transfer Function

The proposed method of designing decentralized controllers for multivariable processes involves three main steps:

1. Design individual controllers by ignoring the loop interaction;

2. Estimate the equivalent transfer function for each individual loop through dynamic interaction analysis;

3. Design decentralized controller based on the equivalent-transfer function.

Let  $\tilde{\mathbf{G}} = \text{diag}\{\mathbf{G}\}$ , and ignore the interaction effect among control loops, the initial controller  $\tilde{\mathbf{C}}$  can be designed by applying the well known IMC tuning rules to each element in  $\tilde{\mathbf{G}}$ .<sup>2</sup> The IMC design procedure is brief studied as follows. The process model  $\tilde{g}$  is factorized into an all-pass portion  $\tilde{g}_+$  and minimum phase portion  $\tilde{g}_-$ , that is

$$\tilde{g} = \tilde{g}_+ \tilde{g}_-$$

The allpass portion  $\tilde{g}_+$  includes all the open right-half-plane zeros, and delays of  $\tilde{g}$  and has the form

$$\tilde{g}_+ = e^{-\theta s} \prod_i (-\beta_i s + 1) \quad \text{Re}\{\beta_i\} > 0$$

where  $\theta > 0$  is the time delay, and  $\beta_i^{-1}$  is the right-half-plane zero in the process model.

Then the IMC controller and the complementary sensitivity function are derived respectively as

$$g_c = \tilde{g}_+^{-1} f$$

and

$$T = \tilde{g}_+ f$$

where  $f$  is the IMC filter, and has the form

$$f = \frac{1}{(\tau_C s + 1)^r}$$

where the filter order  $r$  is selected large enough to make  $g_c$  proper, and the adjustable filter parameter  $\tau_C$  provides the tradeoff between performance and robustness. The key advantage of the IMC design procedure is that all controller parameters are related in a unique, straightforward manner to the model parameters. There is only one adjustable parameter  $\tau_C$  which has intuitive appeal because it determines the speed of response of the system. Furthermore,  $\tau_C$  is approximately proportional to the closed-loop bandwidth, which must always be smaller than the bandwidth over which the process model is valid.

Even though more precise higher-order process models can be obtained by either physical model construction (following the mass and energy balance principles) or the classical parameter identification methods, from a practical point of view, the lower order process model is more convenient for controller design. Six common used low order process models and parameters of their IMC-PID controllers are listed in Table 1, where  $g_{CL}$  and  $\omega_c$  are the close-loop transfer function and the crossover frequency of  $g_c$ , respectively.

From Eq. 13 and according to Table 1, we have

$$\mathbf{P} = \begin{pmatrix} \frac{1 + g_{11}\tilde{c}_1}{g_{11}\tilde{c}_1} & 1 & \cdots & 1 \\ 1 & \frac{1 + g_{22}\tilde{c}_2}{g_{22}\tilde{c}_2} & \cdots & 1 \\ \vdots & \vdots & \ddots & \vdots \\ 1 & 1 & \cdots & \frac{1 + g_{nn}\tilde{c}_n}{g_{nn}\tilde{c}_n} \end{pmatrix}$$



**Table 1. Parameters of IMC-PID Controller for Typical Low-Order Systems<sup>a</sup>**

	$g$	$g_{CL}$	$\omega_c$	$k_P$	$\tau_I$	$\tau_D^b$
A <sup>c</sup>	$ke^{-\theta s}$			—	$k_I$	—
B	$\frac{ke^{-\theta s}}{s}$			$\frac{1}{k(\tau_C + \theta)}$	—	—
C	$\frac{ke^{-\theta s}}{\tau s + 1}$	$\frac{e^{-\theta s}}{\tau_C s + 1}$	$\frac{1}{\tau_C + \theta}$	$\frac{\tau}{k(\tau_C + \theta)}$	$\tau$	—
D	$\frac{ke^{-\theta s}}{s(\tau s + 1)}$			$\frac{1}{k(\tau_C + \theta)}$	—	$\tau$
E	$\frac{ke^{-\theta s}}{(\tau s + 1)(\tau' s + 1)}$			$\frac{\tau + \tau'}{k(\tau_C + \theta)}$	$\tau + \tau'$	$\frac{\tau\tau'}{\tau + \tau'}$
F	$\frac{ke^{-\theta s}}{\tau^2 s + 2\xi\tau s + 1}$			$\frac{2\xi\tau}{k(\tau_C + \theta)}$	$2\xi\tau$	$\frac{\tau}{2\xi}$

<sup>a</sup>The given settings are IAE and ISE optimal for step setpoint changes when  $\tau_C = 0$  and  $\tau_C = \theta$  respectively. It is recommended to select  $\tau_C > \theta$  for practical design.

<sup>b</sup>To achieve much better performance, the derivation can be added by following tranditional rule.<sup>24</sup>

<sup>c</sup>For pure time delay system, the pure integral controller  $c(s) = (k_I/s)$  is applied and  $k_I \equiv (k_P/\tau_I) = [1/k(\tau_C + \theta)]$ .<sup>4</sup>

$$= \begin{pmatrix} g_{11,CL}^{-1} & 1 & \cdots & 1 \\ 1 & g_{22,CL}^{-1} & \cdots & 1 \\ \vdots & \vdots & \ddots & \vdots \\ 1 & 1 & \cdots & g_{nn,CL}^{-1} \end{pmatrix}$$

$$= \begin{pmatrix} (\tilde{\tau}_{C1}s + 1)e^{\theta_{11}s} & 1 & \cdots & 1 \\ 1 & (\tilde{\tau}_{C2}s + 1)e^{\theta_{22}s} & \cdots & 1 \\ \vdots & \vdots & \ddots & \vdots \\ 1 & 1 & \cdots & (\tilde{\tau}_{Cn}s + 1)e^{\theta_{nn}s} \end{pmatrix}. \quad (16)$$

Since each controller is designed around the critical frequency of its transfer function, the dRI of individual control loop  $y_i - u_i$  can be estimated at the critical frequency  $j\omega_{cri}$

$$\phi_{ii,n-1}(j\omega_{cri}) = \|\mathbf{G}\mathbf{g}_{ii,n-1}(j\omega_{cri}) \otimes (\mathbf{G}^{ii}(j\omega_{cri}) \otimes \mathbf{P}^{ii}(j\omega_{cri}))^{-T}\|_{\Sigma} \quad (17)$$

For interactive multivariable process  $\mathbf{G}$ , it is desirable to have the same open-loop transfer function as multivariable control system  $\tilde{\mathbf{G}}\tilde{\mathbf{C}}$ .<sup>13</sup> As controller  $\tilde{\mathbf{C}}$  is designed for the diagonal elements of  $\mathbf{G}$  without considering the couplings between control loops, the designed controller should be detuned by

$$c_i = \frac{\tilde{c}_i}{\rho_{ii,n-1}} = \frac{\tilde{c}_i}{1 + \phi_{ii,n-1}}$$

to result approximately the same closed-loop control performance. However, it is impractical to use  $\rho_{ii,n-1}$  directly to fine-tune the controller, because it has different values at different frequencies. To solve this problem, one possible way is to use some appropriate transfer functions to identify those MMFs. Since at the neighborhood of the critical point, the transmission interaction can be considered as a linear function, it is reasonable to represent the MMF by a low-order transfer function involved the first two items of its Taylor series, which can be further simplified for controller design by a pure-time delay transfer function as

$$\rho_{ii,n-1} = k_{\rho_{ii,n-1}} e^{-\theta_{\rho_{ii,n-1}} s}, \quad (18)$$

where

$$k_{\rho_{ii,n-1}} = |\rho_{ii,n-1}(j\omega_{cri})| = |1 + \phi_{ii,n-1}(j\omega_{cri})| \quad (19)$$

and

$$\theta_{\rho_{ii,n-1}} = -\frac{\arg(\rho_{ii,n-1}(j\omega_{cri}))}{\omega_{cri}} = -\frac{\arg(1 + \phi_{ii,n-1}(j\omega_{cri}))}{\omega_{cri}} \quad (20)$$

with  $\omega_{cri}$  indicates the critical frequency of the  $i$ th control loop  $y_i - u_i$ . Then for individual control loop  $y_i - u_i$  with an arbitrary process model listed in Table 1, its equivalent transfer function can be represented as showed by the third column in Table 2, where

$$f_{ki} = \max\{1, k_{\rho_{ii,n-1}}\}, \quad (21)$$

and

$$f_{\theta i} = \max\left\{1, 1 + \frac{\theta_{\rho_{ii,n-1}}}{\theta_{ii}}\right\}. \quad (22)$$

**Remark 3:** Since the region between  $\tilde{\omega}_{ci}$  ( $|g_{ii}\tilde{c}_i| = 1$ ) and  $\tilde{\omega}_{180}$  ( $\arg(g_{ii}\tilde{c}_i) = -180^\circ$ ) is most critical for individual control loop design, the crossover frequency of ( $g_{ii}\tilde{c}_i$ ) can be adopted as the critical frequency point for determining the dRI to the particular loop  $y_i - u_i$  to obtain  $\hat{g}_{ii}$ .<sup>25</sup>

**Remark 4:** In Eqs. 21 and 22, the factors  $f_{ki}$  and  $f_{\theta i}$  are selected to be not smaller than 1, such that the equivalent open loop gain and the time delay of  $\hat{g}_{ii}$  are no smaller than that of  $g_{ii}$ . The reason for such selection is to make the resultant controller settings more conservative than that of  $\hat{g}_{ii}$ , such that loop failure tolerance property can be preserved.

**Table 2.** PID Controllers of the Equivalent Processes for Typical Low-Order Systems

	$g_{ii}$	$\hat{g}_{ii}$	$k_P$	$\tau_I$	$\tau_D$
A <sup>a</sup>	$k_{ii}e^{-\theta_{ii}s}$	$f_{ki}k_{ii}e^{-f_{\theta i}\theta_{ii}s}$	—	$k_{Ii}$	—
B	$\frac{k_{ii}e^{-\theta_{ii}s}}{s}$	$\frac{f_{ki}k_{ii}e^{-f_{\theta i}\theta_{ii}s}}{s}$	$\frac{1}{f_{ki}k_{ii}(\tau_{Ci} + f_{\theta i}\theta_{ii})}$	—	—
C	$\frac{k_{ii}e^{-\theta_{ii}s}}{\tau_{ii}s + 1}$	$\frac{f_{ki}k_{ii}e^{-f_{\theta i}\theta_{ii}s}}{\tau_{ii}s + 1}$	$\frac{\tau_{ii}}{f_{ki}k_{ii}(\tau_{Ci} + f_{\theta i}\theta_{ii})}$	$\tau_{ii}$	—
D	$\frac{k_{ii}e^{-\theta_{ii}s}}{s(\tau_{ii}s + 1)}$	$\frac{f_{ki}k_{ii}e^{-f_{\theta i}\theta_{ii}s}}{s(\tau_{ii}s + 1)}$	$\frac{1}{f_{ki}k_{ii}(\tau_{Ci} + f_{\theta i}\theta_{ii})}$	—	$\tau_{ii}$
E	$\frac{k_{ii}e^{-\theta_{ii}s}}{(\tau_{ii}s + 1)(\tau'_{ii}s + 1)}$	$\frac{f_{ki}k_{ii}e^{-f_{\theta i}\theta_{ii}s}}{(\tau_{ii}s + 1)(\tau'_{ii}s + 1)}$	$\frac{\tau_{ii} + \tau'_{ii}}{f_{ki}k_{ii}(\tau_{Ci} + f_{\theta i}\theta_{ii})}$	$\tau_{ii} + \tau'_{ii}$	$\frac{\tau_{ii}\tau'_{ii}}{\tau_{ii} + \tau'_{ii}}$
F <sup>b</sup>	$\frac{k_{ii}e^{-\theta_{ii}s}}{\tau_{ii}^2s + 2\xi_{ii}\tau_{ii}s + 1}$	$\frac{f_{ki}k_{ii}e^{-f_{\theta i}\theta_{ii}s}}{\tau_{ii}^2s + 2\xi_{ii}\tau_{ii}s + 1}$	$\frac{2\xi_{ii}\tau_{ii}}{f_{ki}k_{ii}(\tau_{Ci} + f_{\theta i}\theta_{ii})}$	$2\xi_{ii}\tau_{ii}$	$\frac{\tau_{ii}}{2\xi_{ii}}$

<sup>a</sup>For pure time delay system, the pure integral controller  $c(s) = (k_I/s)$  is applied and  $k_{Ii} \equiv (k_P/\tau_{Ii}) = [1/f_{ki}k_{ii}(\tau_{Ci} + f_{\theta i}\theta_{ii})]$ .

## Design of Decentralized Controller

Once the closed-loop properties of the diagonal elements, and the critical frequencies of all individual control loops are determined, the dRI and MMF can be obtained through calculating the matrix **P** and dDRIA. Then, the parameters of decentralized controllers can be calculated based on the equivalent-transfer function of each control loop, and the IMC-PID tuning rules as shown in Table 2.

In such design procedure, the overall control system stability is assured if the loop pairing is structurally stable which can be explained as follows:

1. Each  $\tilde{c}_i$  designed without considering loop interaction is more aggressive to control loop  $y_i - u_i$  than that of the final control setting  $c_i$ . Generally, we have  $\bar{\sigma}(\Delta_1) \leq \bar{\sigma}(\Delta_2)$  as  $\max\{1, |\rho_{ii,n-1}|\} \geq 1$ , where  $\bar{\sigma}(\mathbf{A})$  is the maximum singular value of matrix **A**,  $\Delta_1 = \tilde{\mathbf{G}}\mathbf{C}(1 + \tilde{\mathbf{G}}\mathbf{C})^{-1}$  and  $\Delta_2 = \tilde{\mathbf{G}}\tilde{\mathbf{C}}(1 + \tilde{\mathbf{G}}\tilde{\mathbf{C}})^{-1}$ .

2. Let  $\mathbf{M} = -(\mathbf{G} - \tilde{\mathbf{G}})\tilde{\mathbf{G}}^{-1}$ , and following the definition of the structured singular value (SSV)<sup>26</sup>

$$\mu_{\Delta}(\mathbf{M}) \equiv \frac{1}{\min\{\bar{\sigma}(\Delta)|\det(\mathbf{I} - k_m\mathbf{M}\Delta) = 0 \text{ for structured } \Delta\}},$$

we have  $\mu_{\Delta_1}(\mathbf{M}) \leq \mu_{\Delta_2}(\mathbf{M})$ , which implies there exist smaller interactions among control loops when the detuned controller **C** is applied.<sup>13</sup>

3. Since the bigger dRI  $\phi_{ii,n-1}$  is used to determine the detuning factors, and  $f_{ki}$  and  $f_{\theta i}$  are no smaller than 1, the resultant controller  $c_i$  will be more conservative with smaller gain and crossover frequency compared with  $\tilde{c}_i$ .

4. Conservative control action in each loop presents smaller interaction to other loops. As the design based on  $\hat{g}_{ii}$  for loop  $y_i - u_i$  will end up with a more conservative  $c_i$ . The stability margin for each individual loop will be further increased compared with using the true  $\phi_{ii,n-1}$ .

Summarize the above results, a procedure for designing decentralized PID controller for general multivariable processes is illustrated as in Figure 4.

**Remark 5:** As the interactions among control loops are ignored in both the dynamic interaction estimation step and the PID controller designing step, all available SISO PID controller design techniques can be adopted. Thus, according to the expected control performance, one can select the most suitable

tuning rules, such as Ziegler and Nichols tuning rule,<sup>1</sup> IMC tuning rule,<sup>2</sup> and some other optimal design methods<sup>3</sup> for each step independently. Apparently, applying various tuning rules must lead to various interaction estimations, initial controller settings, final controller settings, as well as overall control performance. However, has no influence to the design mechanism of our method. In the present article, the IMC-PID tuning rule is adopted because of its robust, generally good responses for setpoint changes and widely accepted.

## Simulation Examples

To evaluate effectiveness of the proposed decentralized PID controller design method, 10 multivariable processes in reference<sup>5</sup> are studied:

- $2 \times 2$  systems: (1) Tyreus stabilizer—TS; (2) Wood and

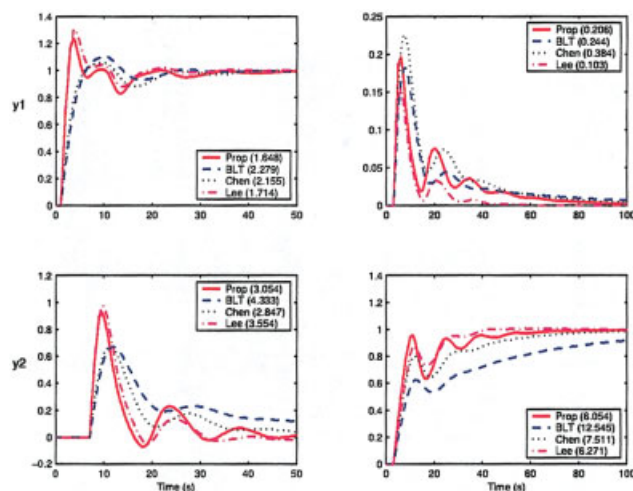


**Figure 6.** Step response and ISE values of decentralized control for Wood and Berry (lower) systems (solid line: Proposed design, dashed line: BLT design, dashed-dotted line: Lee et al., dotted line: Chen et al.).

[Color figure can be viewed in the online issue, which is available at [www.interscience.wiley.com](http://www.interscience.wiley.com).]

**Table 3. Parameters of the Decentralized PID Controllers for 10 Classical Systems<sup>a</sup>**

	BLT design		Lee et al. design		Chen et al. design		Proposed design		
	$k_P$	$\tau_I$	$k_P$	$\tau_I$	$k_P$	$\tau_I$	$k_P$	$\tau_I$	$\tau_D$
TS	-16.6	20.6					-149.0	3.460	2.300
	70.6	80.1					769.5	64.00	13.75
WB	0.375	8.29	0.850	7.21	0.436	11.0	0.932	16.70	—
	-0.075	23.6	-0.0885	8.86	-0.0945	15.5	-0.124	14.40	—
VL	-1.07	7.1	-1.31	2.26	1.21	4.64	-2.121	7.000	—
	1.97	2.58	3.97	2.42	3.74	1.10	3.951	9.200	—
WW	27.4	41.4	53.8	31.1			52.52	60.00	—
	-13.3	52.9	-20.3	29.7			-24.52	35.00	—
OR	1.51	16.4					1.676	6.700	—
	-0.295	18					-0.353	5.000	—
	2.63	6.61					4.385	8.620	—
T1	-17.8	4.5					-20.85	66.67	—
	0.749	5.61					1.168	2.860	0.715
T4	-0.261	139					-0.088	33.30	—
	-11.26	7.09					-23.64	66.67	—
	-3.52	14.5					0.622	2.860	0.715
DL	-0.182	15.1					-0.515	46.48	11.57
	-0.118	23.5					-0.410	43.48	10.87
	-7.26	11					-23.64	66.67	—
A1	0.429	12.1					0.589	2.860	0.715
	0.743	7.94					0.028	1.000	—
	2.28	72.2	0.385	34.72	0.176	62.9	3.698	61.00	14.75
	2.94	7.48	6.190	21.80	0.220	31.0	4.481	32.00	—
A2	1.18	7.39	2.836	19.22	3.150	8.03	1.666	16.20	—
	2.02	27.8	0.732	36.93	0.447	47.5	4.821	53.00	4.528
	0.923	61.7					3.884	41.30	6.632
	1.16	13.2					2.549	44.60	—
	0.727	13.2					1.311	18.50	—
	2.17	40					4.233	54.30	5.569

<sup>a</sup>In the proposed design, the control configurations of both Tyreus case 4 and Doukas and Luyben systems are re-selected as  $y_1 - u_1/y_2 - u_3/y_3 - u_2$  and  $y_1 - u_4/y_2 - u_2/y_3 - u_1/y_4 - u_3$ , respectively, by using the pairing method proposed in ref.<sup>19</sup>.

Berry—WB; (3) Vinante and Luyben—VL; (4) Wardle and Wood—WW.

•  $3 \times 3$  systems: (5) Ogunnaike and Ray—OR; (6) Tyreus case 1—T1; (7) Tyreus case 4—T4.

•  $4 \times 4$  systems: (8) Doukas and Luyben—DL; (9) Alatiqi case 1—A1; (10) Alatiqi case 2—A2.

The process open-loop transfer function matrices of these systems are listed by Tables A1, A2 and A3, respectively, in Appendix. As some process models, such as  $g_{11}$  in TS case, are in higher-order (higher than second-order), the standard order reduction method is used to make them have the forms as those presented in Table 1. The controller parameters are listed in Table 3 together with those obtained by using other three design methods: the biggest log-modulus tuning (BLT) method of Luyben,<sup>5</sup> the trial-and-error method,<sup>15</sup> and an independent design method based on Nyquist stability analysis.<sup>14</sup> It should be pointed out that the Gershgorin circle and Gershgorin band are utilized to determine the stability region in the last method, a static decoupler is required if the processes is not open-loop column diagonal dominance.

To evaluate the output control performance, we consider a unit step setpoint change ( $r_i = 1$ ) of all control loops one-by-one, and the integral square error (ISE) of  $e_i = y_i - r_i$  is used to evaluate the control performance

$$J_i = \int_0^{\infty} e_i^2 dt.$$

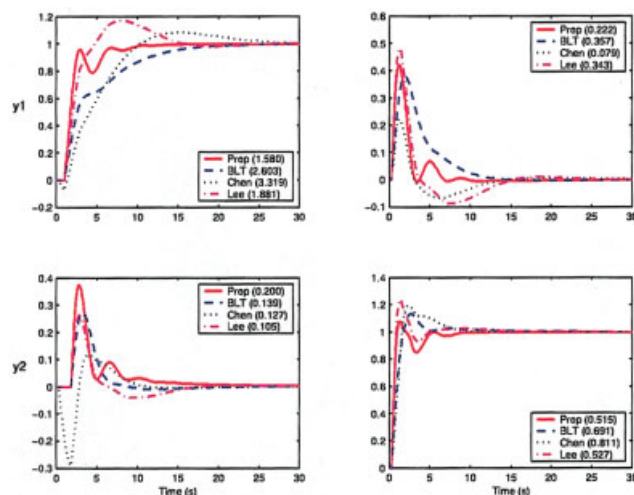


**Figure 7. Step response and ISE values of decentralized control for Vinante and Luyben system (solid line: Proposed design, dashed line: BLT design, dashed-dotted line: Lee et al., dotted line: Chen et al.).**

[Color figure can be viewed in the online issue, which is available at [www.interscience.wiley.com](http://www.interscience.wiley.com).]



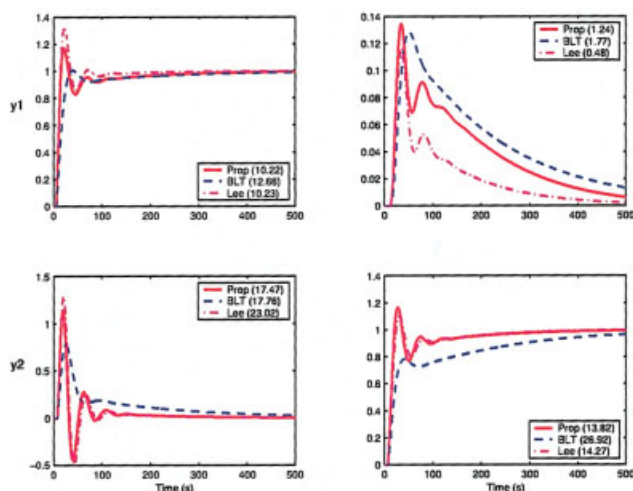


**Figure 8.** Step response and ISE values of decentralized control for Wardle and Wood system (solid line: Proposed design, dashed line: BLT design, dashed-dotted line: Lee et al., dotted line: Chen et al.).

[Color figure can be viewed in the online issue, which is available at [www.interscience.wiley.com](http://www.interscience.wiley.com).]

The simulation results and ISE values are given in Figures 5-14. The results show that, for some of the  $2 \times 2$  processes, the proposed design provides better performance than both BLT method and Chen et al. method, and is quite competitive with Lee et al. method, but for higher dimensional processes, the proposed design provides less conservative controller settings, as well as better control performance.

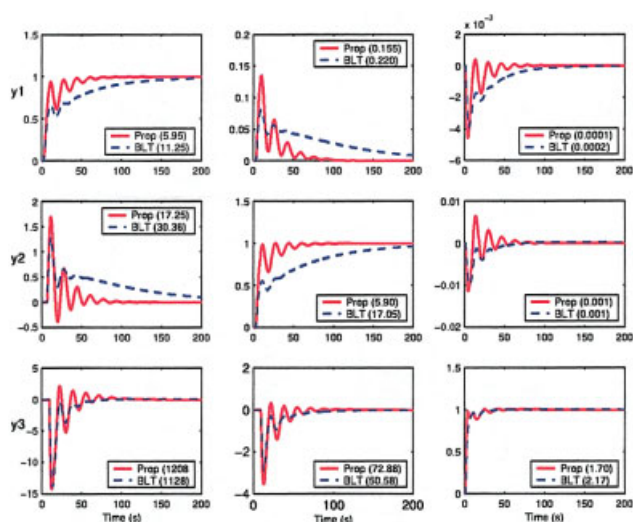


**Figure 9.** Step response and ISE values of decentralized control for Ogunnaile and Ray system (solid line: Proposed design, dashed line: BLT design).

[Color figure can be viewed in the online issue, which is available at [www.interscience.wiley.com](http://www.interscience.wiley.com).]

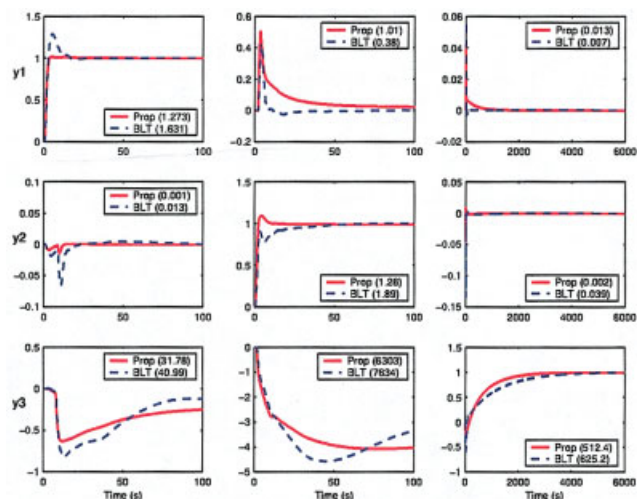


**Figure 10.** Step response and ISE values of decentralized control for Tyreus case 1 systems (solid line: Proposed design, dashed line: BLT design).

[Color figure can be viewed in the online issue, which is available at [www.interscience.wiley.com](http://www.interscience.wiley.com).]

## Conclusion

A simple yet effective design method for decentralized PID controller design method was proposed, based on dynamic interaction analysis and internal model control principle. On the basis of structure decomposition, the dynamic relative interaction was defined and represented by the process model and controller explicitly. An initial decentralized controller was designed first by using the diagonal elements and then implemented to estimate the dRI to individual control loop from all others. By using the dRI, the MMF was derived and simplified

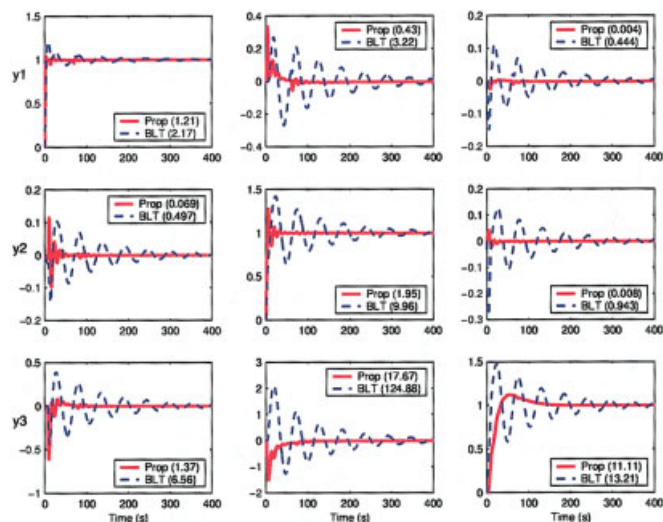


**Figure 11.** Step response and ISE values of decentralized control for Tyreus case 4 system (solid line: Proposed design, dashed line: BLT design).

[Color figure can be viewed in the online issue, which is available at [www.interscience.wiley.com](http://www.interscience.wiley.com).]

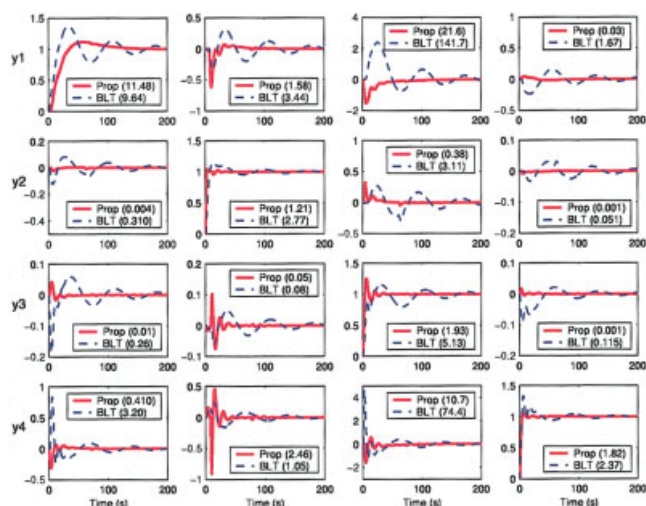


**Figure 12.** Step response and ISE values of decentralized control for Doukas and Luyben system (solid line: Proposed design, dashed line: BLT design).

[Color figure can be viewed in the online issue, which is available at [www.interscience.wiley.com](http://www.interscience.wiley.com).]

to a pure time delay function at the neighborhood of each control loop critical frequency to obtain the equivalent transfer function. Consequently, by applying the IMC-PID tuning rules for the equivalent-transfer function, appropriate controller parameters for individual control loop were determined. The proposed technique is very simple and effective, and has been applied to a variety of  $2 \times 2$ ,  $3 \times 3$ , and  $4 \times 4$  systems. Simulation results showed that the overall control system performance is much better than that of other tuning methods,

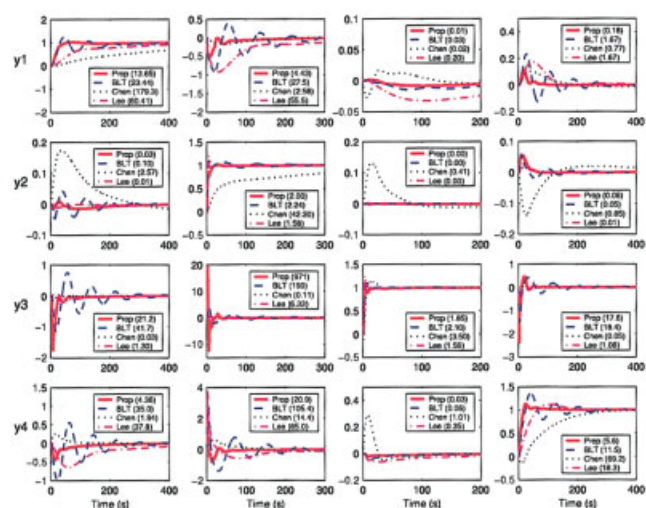


**Figure 13.** Step response and ISE values of decentralized control for Alatiqi case 1 system (solid line: Proposed design, dashed line: BLT design, dashed-dotted line: Lee et al., dotted line: Chen et al.).

[Color figure can be viewed in the online issue, which is available at [www.interscience.wiley.com](http://www.interscience.wiley.com).]

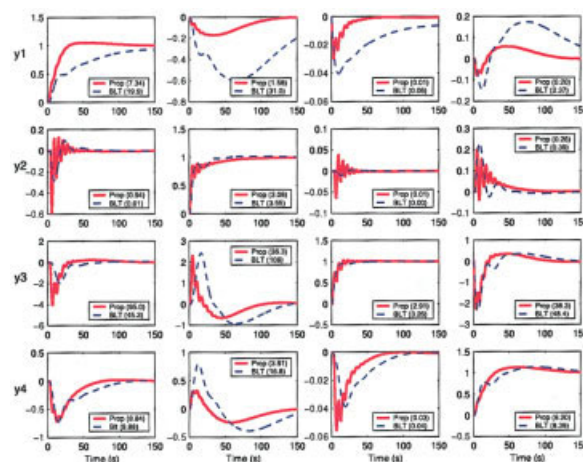


**Figure 14.** Step response and ISE values of decentralized control for Alatiqi case 2 system (solid line: Proposed design, dashed line: BLT design).

[Color figure can be viewed in the online issue, which is available at [www.interscience.wiley.com](http://www.interscience.wiley.com).]

such as the BLT method, the trial and error method, and the independent design method, based on Nyquist stability analysis, especially for higher-dimensional processes.

Since the intention of this article is to present a simple and effective design method of decentralized PID controller for general multivariable processes, the decentralized closed-loop integrity was not considered here. As an important potential advantage for decentralized control structure,<sup>27,28,29</sup> this issue is currently under study and will be discussed in the next report.

## Literature Cited

1. Ziegler JG, Nichols NB. Optimum settings for automatic controllers. *Trans ASME*. 1942;64:759–768.
2. Rivera DE, Morari M, Skogestad S. Internal model control. 4. PID controller design. *Ind Eng Chem Process Des Dev*. 1986;25:252–265.
3. Åström KJ, Hägglund TH. *PID Controllers: Theory, Design and Tuning* (2nd ed.). Instrument Society of America: Research Triangle Park, NC; 1995.
4. Skogestad S. Simple analytic rules for model reduction and PID controller tuning. *J of Proc Control*. 2003;13:291–309.
5. Luyben WL. Simple method for tuning SISO controllers in multivariable systems. *Ind Eng Chem Proc Des Dev*. 1986;25:654–660.
6. Monica TJ, Yu CC, Luyben WL. Improved multiloop single-input/single-output (SISO) controllers for multivariable processes. *Ind Eng Chem Res*. 1988;27:969–973.
7. Chien IL, Huang HP, Yang JC. A simple multiloop tuning method for PID controllers with no proportional kick. *Ind Eng Chem Res*. 1999;38:1456–1468.
8. Lee J, Edgar TF. Multiloop PI/PID control system improvement via adjusting the dominant pole or the peak amplitude ratio. *Chem Eng Sci*. 2006;61:1658–1666.
9. Hovd M, Skogestad S. Sequential design of decentralized controllers. *Automatica*. 1994;30:1601–1607.
10. Shiu SJ, Hwang SH. Sequential design method for multivariable decoupling and multiloop PID controllers. *Ind Eng Chem Res*. 1998;37:107–119.
11. Economou M, Morari M. Internal model control: 6. multiloop design. *Ind Eng Chem Proc Des Dev*. 1986;25:411–419.
12. Hovd M, Skogestad S. Improved independent design of robust decentralized controllers. *J of Proc Control*. 1993;3:43–51.
13. Grosdidier P, Morari M. Interaction measures for systems under decentralized control. *Automatica*. 1986;22:309–319.

14. Chen D, Seborg DE. Design of decentralized PI control systems based on Nyquist stability analysis. *J of Proc Control*. 2003;13:27–39.
15. Lee J, Cho W, Edgar TF. Multiloop PI controller tuning for interaction multivariable processes. *Computers and Chem Eng*. 1998;22:1711–1723.
16. Wang QG, Lee TH, Zhang Y. Multi-loop version of the modified ZieglerNichols method for two input two output process. *Ind Eng Chem Res*. 1998;37:4725–4733.
17. Huang HP, Jeng JC, Chiang CH, Pan W. A direct method for multi-loop PI/PID controller design. *J of Proc Control*. 2003;13:769–786.
18. Bristol EH. On a Philosophy of Interaction in a Multiloop World. *ISA Chemical & Petroleum Division Chempid Symposium*. St. Louis, Missouri; May; 1967.
19. He MJ, Cai WJ. New criterion for control loop configuration of multivariable processes. *Ind Eng Chem Res*. 2004;43:7057–7064.
20. Witcher M, McAvoy TJ. Interacting control systems: Steady state and dynamic measurement of interactions. *ISA Trans*. 1977;16:35–41.
21. Tung L, Edgar TF. Analysis of control output interactions in dynamic systems. *AIChE J*. 1981;27:690–693.
22. McAvoy TJ, Arkun Y, Chen R, Robinson D, Schnelle PD. A new approach to defining a dynamic relative gain. *Control Eng Practice*. 2003;11:907–914.
23. Lee J, Edgar TF. Dynamic interaction measures for decentralized control of multivariable processes. *Ind Eng Chem Res*. 2004;43:283–287.
24. Ingimundarson A, Hägglund T. Performance comparison between PID and dead-time compensating controllers. *J of Process Control*. 2002;12:887–895.
25. Skogestad S, Postlethwaite I. *Multivariable Feedback Control*. John Wiley and Sons: New York; 1996.
26. Doyle JC. Analysis of feedback systems with structured uncertainties. *IEEE Proceedings Part D*. 1982;129:242–250.
27. Chiu MS, Arkun Y. Decentralized control structure selection based on integrity considerations. *Ind Eng Chem Res*. 1990;29:369–373.
28. Campo PJ, Morari M. Achievable closed-loop properties of systems under decentralized control: Conditions involving the steady-state gain. *IEEE Trans Autom Control*. 1994;39:932–943.
29. He MJ, Cai WJ, Li SY. Evaluation of decentralized closed-loop integrity for multivariable control system. *Ind Eng Chem Res*. 2005;44:3567–3574.

## Appendix: The Transfer Function Matrices of Studied Systems

**Table A1. Process Open-Loop Transfer Functions of  $2 \times 2$  Systems**

	TS (Tyreus stabilizer)	WB (Wood and Berry)	VL (Vinante and Luyben)	WW (Wardle and Wood)
$g_{11}$	$\frac{-0.1153(10s+1)e^{-0.1s}}{(4s+1)^3}$	$\frac{12.8e^{-s}}{16.7s+1}$	$\frac{-2.2e^{-s}}{7s+1}$	$\frac{0.126e^{-6s}}{60s+1}$
$g_{12}$	$\frac{0.2429e^{-2s}}{(33s+1)^2}$	$\frac{-18.9e^{-3s}}{21s+1}$	$\frac{1.3e^{-0.3s}}{7s+1}$	$\frac{-0.101e^{-12s}}{(48s+1)(45s+1)}$
$g_{21}$	$\frac{-0.0887e^{-12.6s}}{(43s+1)(22s+1)}$	$\frac{6.6e^{-7s}}{10.9s+1}$	$\frac{-2.8e^{-1.8s}}{9.5s+1}$	$\frac{0.094e^{-8s}}{38s+1}$
$g_{22}$	$\frac{0.2429e^{-0.17s}}{(44s+1)(20s+1)}$	$\frac{-19.4e^{-3s}}{14.4s+1}$	$\frac{4.3e^{-0.35s}}{9.2s+1}$	$\frac{-0.12e^{-8s}}{35s+1}$

**Table A2. Process Open-Loop Transfer Functions of  $3 \times 3$  Systems**

	OR (Ogunnaike and Ray)	T1 (Tyreus case 1)	T4 (Tyreus case 4)
$g_{11}$	$\frac{0.66e^{-2.6s}}{6.7s+1}$	$\frac{-1.986e^{-0.71s}}{66.67s+1}$	$\frac{-1.986e^{-0.71s}}{66.67s+1}$
$g_{12}$	$\frac{-0.61e^{-3.5s}}{8.64s+1}$	$\frac{5.984e^{-2.24s}}{14.29s+1}$	$\frac{5.24e^{-60s}}{400s+1}$
$g_{13}$	$\frac{-0.0049e^{-s}}{9.06s+1}$	$\frac{0.422e^{-8.72s}}{(250s+1)^2}$	$\frac{5.984e^{-2.24s}}{14.29s+1}$
$g_{21}$	$\frac{1.11e^{-6.5s}}{3.25s+1}$	$\frac{0.0204e^{-0.59s}}{(7.14s+1)^2}$	$\frac{0.0204e^{-0.59s}}{(7.14s+1)^2}$
$g_{22}$	$\frac{-2.36e^{-3s}}{5s+1}$	$\frac{2.38e^{-0.42s}}{(1.43s+1)^2}$	$\frac{-0.33e^{-0.68s}}{(2.38s+1)^2}$
$g_{23}$	$\frac{-0.01e^{-1.2s}}{7.09s+1}$	$\frac{0.513e^{-1s}}{(1.43s+1)^2}$	$\frac{2.38e^{-0.42s}}{(1.43s+1)^2}$
$g_{31}$	$\frac{-34.68e^{-9.2s}}{8.15s+1}$	$\frac{0.374e^{-7.75s}}{22.22s+1}$	$\frac{0.374e^{-7.75s}}{22.22s+1}$
$g_{32}$	$\frac{46.2e^{-9.4s}}{10.9s+1}$	$\frac{-9.811e^{-1.59s}}{11.36s+1}$	$\frac{-11.3e^{-3.79s}}{(21.74s+1)^2}$
$g_{33}$	$\frac{0.87(11.61s+1)e^{-s}}{(3.89s+1)(18.8s+1)}$	$\frac{-2.368e^{-27.33s}}{33.3s+1}$	$\frac{-9.811e^{-1.59s}}{11.36s+1}$

**Table A3. Process Open-Loop Transfer Functions of  $4 \times 4$  Systems**

	DL (Doukas and Luyben)	A1 (Alatqi case 1)	A2 (Alatqi case 2)
$g_{11}$	$\frac{-9.811e^{-1.59s}}{11.36s + 1}$	$\frac{2.22e^{-2.5s}}{(36s + 1)(25s + 1)}$	$\frac{4.09e^{-1.3s}}{(33s + 1)(8.3s + 1)}$
$g_{12}$	$\frac{0.374e^{-7.75s}}{22.22s + 1}$	$\frac{-2.94(7.9s + 1)e^{-0.05s}}{(23.7s + 1)^2}$	$\frac{-6.36e^{-0.2s}}{(31.6s + 1)(20s + 1)}$
$g_{13}$	$\frac{-2.368e^{-27.33s}}{33.3s + 1}$	$\frac{0.017e^{-0.2s}}{(31.6s + 1)(7s + 1)}$	$\frac{-0.25e^{-0.4s}}{21s + 1}$
$g_{14}$	$\frac{-11.3e^{-3.79s}}{(21.74s + 1)^2}$	$\frac{-0.64e^{-20s}}{(29s + 1)^2}$	$\frac{-0.49e^{-5s}}{(22s + 1)^2}$
$g_{21}$	$\frac{5.984e^{-2.24s}}{14.29s + 1}$	$\frac{-2.33e^{-5s}}{(35s + 1)^2}$	$\frac{-4.17e^{-4s}}{45s + 1}$
$g_{22}$	$\frac{-1.986e^{-0.71s}}{66.67s + 1}$	$\frac{3.46e^{-1.01s}}{32s + 1}$	$\frac{6.93e^{-1.01s}}{44.6s + 1}$
$g_{23}$	$\frac{0.422e^{-8.72s}}{(250s + 1)^2}$	$\frac{-0.51e^{-7.5s}}{(32s + 1)^2}$	$\frac{-0.05e^{-5s}}{(34.5s + 1)^2}$
$g_{24}$	$\frac{5.24e^{-60s}}{400s + 1}$	$\frac{1.68e^{-2s}}{(28s + 1)^2}$	$\frac{1.53e^{-2.8s}}{48s + 1}$
$g_{31}$	$\frac{2.38e^{-0.42s}}{(1.43s + 1)^2}$	$\frac{-1.06e^{-22s}}{(17s + 1)^2}$	$\frac{-1.73e^{-17s}}{(13s + 1)^2}$
$g_{32}$	$\frac{0.0204e^{-0.59s}}{(7.14s + 1)^2}$	$\frac{3.511e^{-13s}}{(12s + 1)^2}$	$\frac{5.11e^{-11s}}{(13.3s + 1)^2}$
$g_{33}$	$\frac{0.513e^{-s}}{s + 1}$	$\frac{4.41e^{-1.01s}}{16.2s + 1}$	$\frac{4.61e^{-1.02s}}{18.5s + 1}$
$g_{34}$	$\frac{-0.33e^{-0.68s}}{(2.38s + 1)^2}$	$\frac{-5.38e^{-0.5s}}{17s + 1}$	$\frac{-5.48e^{-0.5s}}{15s + 1}$
$g_{41}$	$\frac{-11.3e^{-3.79s}}{(21.74s + 1)^2}$	$\frac{-5.73e^{-2.5s}}{(8s + 1)(50s + 1)}$	$\frac{-11.18e^{-2.6s}}{(43s + 1)(6.5s + 1)}$
$g_{42}$	$\frac{-0.176e^{-0.48s}}{(6.9s + 1)^2}$	$\frac{4.32(25s + 1)e^{-0.01s}}{(50s + 1)(5s + 1)}$	$\frac{14.04e^{-0.02s}}{(45s + 1)(10s + 1)}$
$g_{43}$	$\frac{15.54e^{-s}}{s + 1}$	$\frac{-1.25e^{-2.8s}}{(43.6s + 1)(9s + 1)}$	$\frac{-0.1e^{-0.05s}}{(31.6s + 1)(5s + 1)}$
$g_{44}$	$\frac{4.48e^{-0.52s}}{11.11s + 1}$	$\frac{4.78e^{-1.15s}}{(48s + 1)(5s + 1)}$	$\frac{4.49e^{-0.6s}}{(48s + 1)(6.3s + 1)}$

*Manuscript received Jan. 20, 2006, and revision received July 28, 2006.*